Formation and decay of electron-hole droplets in diamond

J. H. Jiang,[1] M. W. Wu,[1,*] M. Nagai,[2] and M. Kuwata-Gonokami[3]
[1]*Hefei National Laboratory for Physical Sciences at Microscale, University of Science and Technology of China, Hefei, Anhui, 230026, China*
and Department of Physics, University of Science and Technology of China, Hefei, Anhui, 230026, China[†]
[2]*Department of Physics, Kyoto University, Kyoto 606-8502, Japan*
[3]*Department of Applied Physics, University of Tokyo, Hongo, Bunkyo-ku, Tokyo 113-8656, Japan*
(Received 10 August 2004; revised manuscript received 12 November 2004; published 28 January 2005)

We study the formation and decay of electron-hole droplets in diamond at low and high temperatures under different excitations by master equations. The calculation reveals that at low temperature the kinetics of the system is similar to that of a direct semiconductor, whereas at high temperature it is metastable and similar to an indirect semiconductor. Our results at low temperature are consistent with the experimental findings reported by Nagai *et al.* [Phys. Rev. B **68**, 081202(R) (2003)]. The kinetics of the e-h system in diamonds at high temperature under both low and high excitations is also predicted.

DOI: 10.1103/PhysRevB.71.035215 PACS number(s): 71.35.Ee, 81.05.Uw

Photoexcited electron-hole (e-h) systems in semiconductors provide a unique opportunity to understand quantum many-body phenomena with Coulomb interactions. In the dilute density region, an electron and a hole are combined to form a neutral bound state—an exciton. At low temperature, a dense exciton gas condenses into a liquid phase with a metallic character in the form of e-h droplets (EHDs). This macroscopic metallic phase has been extensively investigated in the past three decades in indirect semiconductors such as Ge and Si.[1] The transition between EHD and exciton gas is considered analogous to a classical liquid transition in water, and the EHD formation is well understood with a classical nucleation theory.[2] However, the formation and decay of EHD in photoexcited semiconductors are not only determined by the collection and evaporation of excitons on the surface of EHD but also by carrier recombination. In direct semiconductors in particular, a fast recombination process overcomes the thermal kinetics of carriers. Therefore e-h pairs annihilate before a small e-h ensemble grows to become a macroscopic-size EHD. Consequently, the phase transition is shown to be of second order.[3]

This competition between thermal kinetics and recombination of carriers is also apparent in indirect semiconductors. In traditional indirect semiconductors such as Ge and Si, at a certain high temperature the evaporation rate is larger than the recombination rate, which makes the kinetics of EHD formation similar to that of classical nucleation. In this case, EHD formation exhibits a hysteresis effect and the average drop size is large. However when the temperature is sufficiently low, the thermal kinetics is suppressed. The dominant recombination effect makes the e-h system behave like those in direct semiconductors, i.e., no hysteresis effect and a small average number of pairs per cluster (ANPC). Under this condition the exciton-EHD phase transition changes from first to second order.[3,4] This density and temperature region, where the thermodynamical phase diagram is distorted, is attractive to scientists because the quantum statistics of the quasiparticles is dominant, and a hidden collective phase including Bose-Einstein condensation might appear. In order to understand such a rich variety of macroscopic phases, it is important first to evaluate the kinetics of the liquid-gas transition in the photoexcited indirect semiconductors in the low temperature region. Nevertheless it is not very realistic for conventional indirect semiconductors because of their narrowness in energy scale.

Diamond is a wide band gap indirect semiconductor with a band structure similar to those of Ge and Si, and is a good candidate to study carrier dynamics. Moreover, because of the small dielectric constant of diamond the screening of the Coulomb interaction between carriers is small. Thus one can treat e-h system in diamond in wide energy scale. Recently Shimano *et al.* evaluated the character of EHD in diamond by time-resolved luminescence measurements and reported a higher critical temperature, larger work function, larger density, and shorter lifetime for EHD in diamond compared to Ge and Si.[5] Consistent values are also obtained from an analysis of the luminescence spectra under quasi-cw excitation.[6,7] The dynamics of the EHD formation at 12 K under a different excitation density has also been studied by Nagai *et al.*[8,9] It was observed that after photoexcited carriers are cooled rapidly into a supersaturated exciton gas within several tens of picosecond, spatial condensation of dense exciton gas into EHD occurs within a few hundred picoseconds. In this report we investigate theoretically the kinetics of EHD formation and decay in diamond. First we use a discrete master equation theory developed by Haug and Abraham[10] to investigate the femtosecond excitation in diamond at a low temperature regime where only small e-h clusters are formed. We then use the continuous master equation theory developed by Silver[11] and by Koch and Haug[12] to investigate the dynamics at high temperature regime where the average drop size is too large to be treated discretely. Finally we compare our results with the experimental measurements by Nagai *et al.*[8] The division between the low and high temperature regimes in diamond is $\sim$60 K where the thermal evaporation rate equals to the recombination rate.[13]

For a discrete master equation formalism, if the concentration of clusters containing n e-h pairs at time t is denoted by $f(n,t)$, the master equation describing the evolution of $f(n,t)$ is

TABLE I. EHD and exciton parameters for diamond which are used in the calculation.

	Symbol	Value	Unit	Ref.
Mean EHD lifetime	τ_d	1	ns	5
Mean exciton lifetime	τ_x	100	ns	
Work function of EHD	ϕ	50	meV	5, 7, and 15
Surface energy of EHD	σ_0	1.2	erg/cm^2	16
$\sigma(T)=\sigma_0(1-(T/T_c)^2)$	T_c	165	K	5
Exciton degeneracy	γ	12		
Effective mass of exciton	m_x	7.92	10^{-31} kg	
e-h density of EHD	ρ_0	1.0	10^{20} cm^{-3}	5

$$\frac{\partial}{\partial t}f(n,t) = j_{n-1} - j_n \tag{1}$$

for $n \geqslant 2$, where j_n is the net probability current between the clusters with n and $n+1$ e-h pairs:

$$j_n = g_n f(n,t) - l_{n+1} f(n+1,t). \tag{2}$$

In this equation l_n and g_n are the gain and loss rates of a cluster with n e-h pairs. The gain rate is obtained from the assumption that excitons with a density n_x are collected at the surface of a cluster, and is approximated by $g_n = b n_x n^{2/3}$ with $b = 4\pi R_0^2 v_x$. $R_0 = (3/4\pi\rho_0)^{1/3}$ is the Wigner-Seitz radius of the EHD and $v_x = \sqrt{kT/2\pi m_x}$ is the thermal velocity of excitons with an effective mass m_x. ρ_0 denotes the EHD density. The loss rate is composed of the sum of the evaporation rate α_n and the recombination rate n/τ_n. $l_n = \alpha_n + n/\tau_n$. The evaporation rate is given by a time-independent Richardson-Dushman current, $\alpha_n = b D_x \exp[(-\phi + c\sigma n^{-1/3})/(kT)] n^{2/3}$, where $D_x = \gamma_x (m_x kT/2\pi\hbar^2)^{3/2}$ is the effective density of state of exciton, γ_x is the degeneracy of the exciton ground state and $c\sigma n^{-1/3}$ represents the correction of the binding energy due to surface effect with σ denoting the surface energy of the EHD. These equations are solved together with the continuity equation:

$$\frac{\partial}{\partial t}f(1,t) = G(t) - \sum_{n=1}^{\infty} \frac{n f(n,t)}{\tau_n} - 2j_1 - \sum_{n=2}^{\infty} j_n, \tag{3}$$

with $G(t)$ representing the excitation pulse

$$G(t) = G_0 e^{-(t-t_0)^2/t_p^2}, \tag{4}$$

with t_p standing for the width of laser pulse which is 0.1 ps throughout this paper. It is noted that the coalescence of clusters larger than excitons is neglected.

For the case of high temperature where n is too large to be treated discretely, we turn to the equation of moments.[12] The νth moment of EHD distribution is defined as

$$x_\nu(t) = \int_{n_c}^{\infty} n^\nu f(n,t) dn \tag{5}$$

in which n_c is a critical size where the stationary distribution has a minimum. All clusters smaller than n_c are counted as excitons, while clusters larger than n_c are treated as EHDs. Under this approximation, the "exciton density" is given by

$$n_x(t) = \int_1^{n_c} n f(n,t) dn. \tag{6}$$

Here n_c is calculated approximately by equating loss rate and the gain rate with the recombination loss neglected:

$$\alpha_{n_c} \approx n_x(t) b n_c^{2/3}. \tag{7}$$

The equations of moments are given by

$$\frac{d}{dt}x_0 = J_{n_c} - \left(\frac{d}{dt}n_c\right) f(n_c,t), \tag{8}$$

$$\frac{d}{dt}x_\nu = n_c^\nu \frac{d}{dt}x_0 - \nu\left[\frac{x_\nu}{\tau_d} + x_{\nu-1/3} b (n_s - n_x)\right], \tag{9}$$

with τ_d denoting the mean EHD lifetime and n_s being the saturated exciton density, $n_s = D_x \exp(-\phi/kT)$. $\nu = 1/3,\ 2/3,\ 1,\ 4/3,\ 5/3$, and 2. Finally the continuity equation is

$$\frac{d}{dt}n_x = -\frac{n_x}{\tau_x} - n_c \frac{d}{dt}x_0 + x_{2/3} b (n_s - n_x) + G(t), \tag{10}$$

in which τ_x represents the mean exciton lifetime. The second term describes the change in EHD density and the third term is due to free exciton evaporation and collection by EHD. Equations (8)–(10) form a closed set of equations. The expressions of J_{n_c} and $f(n_c,t)$ in Eq. (8) are given in the Appendix.

We first study the kinetics of the e-h system in diamond at 12 K by using the discrete master equations, under the experimental conditions similar to the ones used by Nagai *et al.*[8] The material parameters are listed in Table I.[14] The results of our calculation are plotted in Figs. 1–4.

In Fig. 1 we present the kinetics under an excitation with $G_0 = 6.6 \times 10^{29}$ cm^{-3} s^{-1} and $t_p = 0.1$ ps which corresponds to a $\sim$0.2 mJ/cm^2 excitation in the experiment.[8,17] The cluster concentration versus time and the number of e-h pairs in a cluster as well as the concentration of some selected clusters versus time are plotted in Figs. 1(a) and 1(b), respectively. The figures indicate that the concentration of small clusters rise faster than that of large cluster because the current j_n in Eq. (1) flows from small clusters to larger ones. It is also seen from the figures that the system reaches quasiequilibrium at about 120 ps and this quasi-equilibrium lasts about 200 ps.

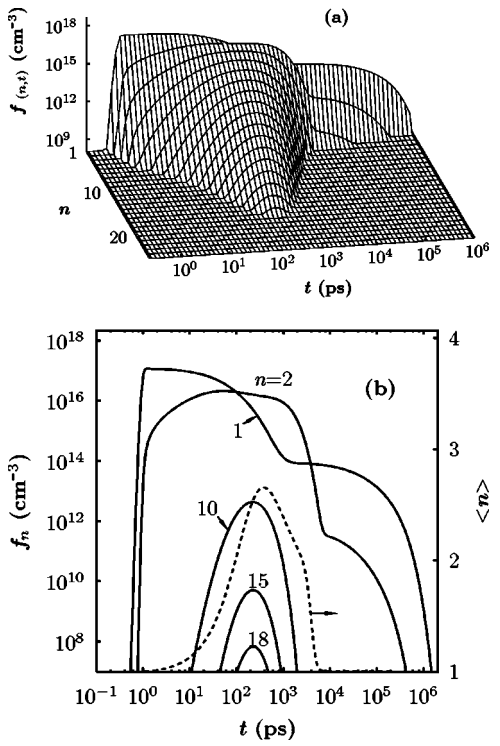

FIG. 1. (a) Cluster concentration versus time and number of e-h pairs per cluster for diamond at $T=12$ K under Gaussian pulse excitation with $G_0=6.6\times10^{29}$ cm^{-3} s^{-1}, $t_p=0.1$ ps, and $t_0=1.0$ ps. (b) Concentration of some selected clusters (solid curve) and ANPC $\langle n\rangle$ (dashed curve) versus time.

In the experiment the peak energy of the EHD emission band shifts toward the low energy side during first 200 ps,[8] which suggests that large clusters are formed at a longer time. Meanwhile from the fact that there is little change of the luminescence in the low energy regime, we conclude that the rate of the formation of small clusters from excitons and the rate of coalescence to large clusters are nearly the same. As a result the concentration of small clusters rises and quickly reaches a steady value. These features are consistent with our calculation. The luminescence indicates that the system reaches its quasiequilibrium in about 200 ps, which is comparable to the 120 ps value we obtained. It is also seen in Fig. 1(b) that excitons ($n=1$) decay much slower than clusters with $n\geqslant2$—because the lifetime of excitons τ_x is larger than that of e-h pairs in e-h clusters τ_d and also because excitons get additional compensation from the recombination of large clusters.

In order to monitor the average size of the cluster, we plot the ANPC $\langle n\rangle=\Sigma_{n=1}^{\infty}nf(n,t)/\Sigma_{n=1}^{\infty}f(n,t)$ as a function of time in Fig. 1(b). The ANPC is less than 3, and is different to that obtained for direct band-gap semiconductors.[10,18] Note that in the present model the coalescence of clusters larger than excitons (e.g., biexcitons) is neglected. The coalescence of clusters adds to the cluster formation mechanism, thus this approximation leads to a smaller ANPC in our results. Despite this, the ANPC is still too small to result in the formation of macroscopic EHDs. The smallness of ANPC and the shortness of the time during which the system is in quasiequilibrium indicate that the system is characteristic of a nonequilibrium, similar to an e-h system in direct semiconductors.

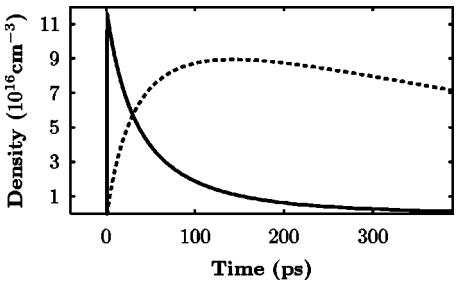

FIG. 2. Exciton density n_x (solid curve) and the total density of e-h pairs in all clusters larger than exciton n_d (dashed curve) for diamond at $T=12$ K under the same excitation as in Fig. 1.

We also show the time evolution of the exciton density n_x and the total density of all e-h pairs condensed in clusters larger than excitons: $n_d=\Sigma_{n=2}^{\infty}nf(n,t)$ in Fig. 2. Thus we can compare the evolution of these densities with that of excitons and the integrated EHD luminescence intensities. We can see that excitons slowly condense into EHDs and n_d reaches a maximum around 150 ps, which corresponds to the 260 ps experimental data.

There are some differences between these densities and the luminescence intensities in the experiment. First, the times when exciton and EHD densities reach their maxima are about one half those in the experiment. This originates partly from the simplified excitation model we use. In this model the only excitations generated by the laser pulse are excitons. In reality, these excitations should be e-h plasma and they are always overheated. After the excitation the e-h system is cooled down in several tens of picoseconds.[8] This relaxation process affects the kinetics of exciton. The absence of this process results in a shorter formation time in the calculation. Second, at the equilibrium stage 90% of the excitation is converted into the EHD phase, while in the experiment only about 50% is converted. This may be partly due to the diffusion of the e-h pairs, and therefore the actual exciton density is smaller than our evaluation. Nevertheless the diffusion effect might be marginal since the time scale is only 300 ps and the initial carrier distribution with a penetration depth of 15 μm is less spatially inhomogeneous. It is reported that the effect of diffusion of an e-h system in Si is negligible during the 200 ps after excitation.[19] Moreover, the high density of e-h pairs causes large Auger recombination in EHD and a repulsion of excitons from EHD by the phonon wind.[20] Thus the efficiency of the collection of excitons which collide with EHD decreases, and less excitons are converted into EHD. These effects also slow down the formation process as the gain rate g_n in Eq. (2) is proportional to exciton density, and thus lead to a longer formation time in the experiment compared to our results.

We now discuss kinetics under a higher excitation. Figure 3 shows the same calculation as in Fig. 1 but with a much higher excitation, i.e., ninety times as large as in Fig. 1. This intensity corresponds to an excitation of ~17 mJ/cm^2 in the experiment.[8] It is seen from the figure that compared to the case of low excitation in Fig. 1, the exciton density decays during the first 20 ps. This explains the absence of exciton

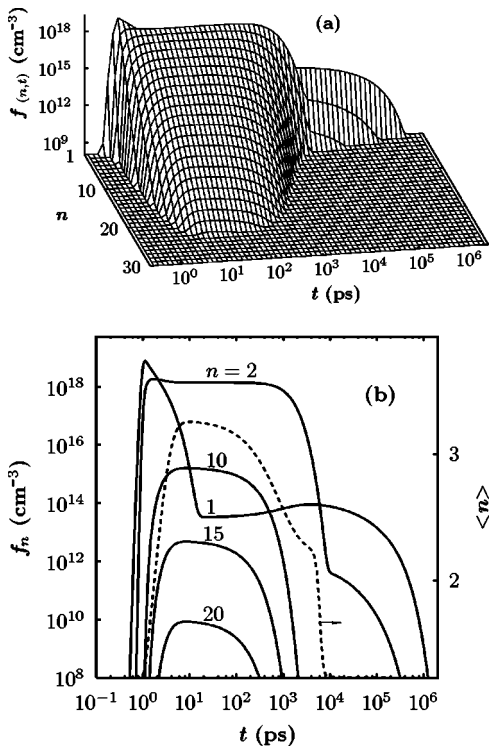

FIG. 3. (a) Cluster concentration versus time and number of e-h pairs per cluster for diamond at $T=12$ K under Gaussian pulse excitation with $G_0=5.6\times10^{31}$ cm^{-3} s^{-1}, $t_p=0.1$ ps, and $t_0=1.0$ ps. (b) Concentration of some selected clusters (solid curve) and ANPC $\langle n\rangle$ (dashed curve) versus time.

luminescence in the experiment performed at a similar excitation.[8] It is also seen that although the peak exciton density is almost proportional to the excitation intensity, the exciton density in the quasi-equilibrium is smaller for larger excitation intensities. In Fig. 1(b) and Fig. 3(b), the exciton density in quasiequilibrium is about 10^{15} cm^{-3} under an excitation of 0.2 mJ/cm^2 and only 10^{13} cm^{-3} under 17 mJ/cm^2. Moreover, the ANPC increases very little despite such a large increase in excitation intensity. This behavior confirms the second-order nature of the exciton-EHD transition at this low temperature, and it is similar to what was discovered in Ge and Si at sufficiently low temperatures.[4] It is understood that the larger excitation intensity makes the concentration of clusters grow up more rapidly since the gain g_n in Eq. (2) is proportional to the exciton density.

Before we discuss the high temperature case, we analyze the dependence on the excitation intensity at low temperature. In Fig. 4 we compare the time delays at which n_d reaches the maximum and half maximum as well as the time delay needed for the exciton density n_x to reach a maximum under different excitation intensities [Fig. 4(a)] with those in the experiment [Fig. 4(b)].[8] The figure shows that our results are in good qualitative agreement with experiment. In both figures the formation time of e-h cluster decreases with the increase of the excitation intensity, and the time when the exciton density (luminescence intensity) reaches its maximum is independent of the excitation intensity. One may find that the time of the maximum density of exciton in our results is nearly zero which is smaller than the experimental value around 20 ps. This is due to the fact that we use a simple model of Gaussian excitation in which the relaxation process of the e-h system is neglected. As mentioned before, the relaxation, diffusion, and the Auger processes slow down the EHD formation process. Thus our calculations produce a relatively small formation time.

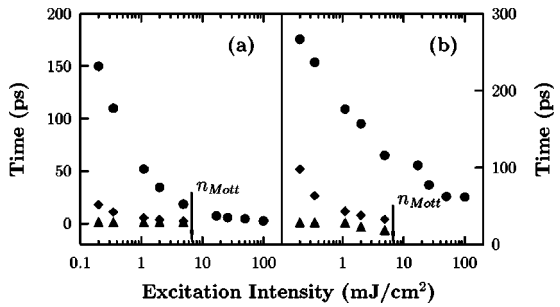

FIG. 4. Calculated (a) and experimental (b) e-h droplet formation times and exciton formation times versus the excitation intensity. ●: time used when n_d reaches its maximum; ◆: time used when n_d reaches its half maximum; ▲: time used when n_x reaches its maximum.

We now study the kinetics of diamond at high temperature (100 K) using equations of moment Eqs. (8)–(10). It is noted that this method only allows one to study the formation and decay processes close to the steady state. We follow the path used for the low temperature case, i.e., first a small excitation and then a high excitation.

In Fig. 5(a) we present the evolution of the "exciton density" Eq. (6), the three integer moments of the EHD distribution Eq. (5), the average size of EHD $\overline{n}=x_1/x_0$ and the relative mean square of EHD distribution

$$\overline{(\Delta n)^2} = [x_2/x_0 - (x_1/x_0)^2]/(x_1/x_0)^2 \tag{11}$$

under an excitation of 1.8 mJ/cm^2. Very different from the results at low temperature where only small clusters are formed, here one finds that the average drop size is very large: about 10^7. Nevertheless the density of all e-h pairs which are condensed in EHDs, i.e., x_1, is rather small, less than 10^{13} cm^{-3}. This can be understood easily: For a high temperature the evaporation rate α_n is much larger and this larger evaporation impedes the formation of EHD. For the same reason the formation of EHD slows down. The time when EHD density reaches its maximum is about 10^4 ps compared to about 40 ps under the same excitation at 12 K. The relative mean square of EHD distribution $\overline{(\Delta n)^2}$, which describes the fluctuation of droplet distribution, is very small when the system is in the steady state.

The kinetics at a higher excitation intensity of 6.1 mJ/cm^2 is plotted in Fig. 5(b). Note that the curve of x_1 in Fig. 5(b) is comparable with that in Fig. 4(b) of Ref. 5—where the excitation density and temperature are similar to those in the calculation—except that our result is plotted in a logarithmic scale and in a larger time range. Moreover the kinetics shows two main differences from the low excitation case: First, the average drop size $\overline{n}$ is much smaller: about 10^4; Second, the

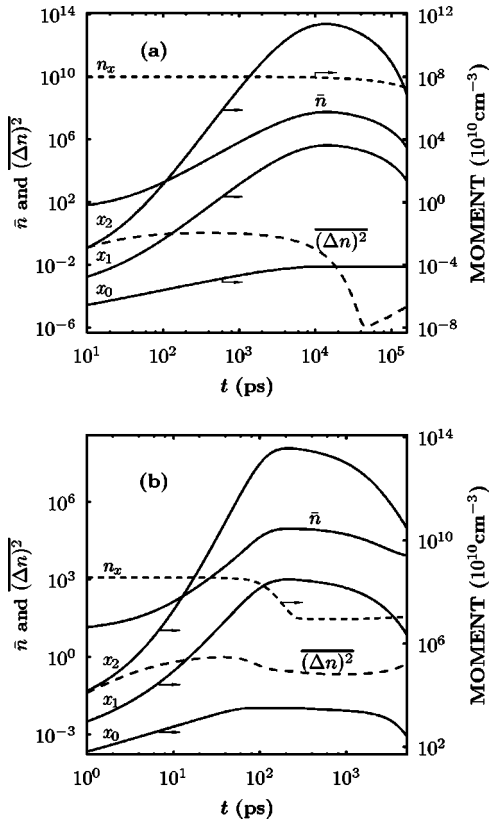

FIG. 5. Time dependence of the "exciton density" n_x, the moments of EHD distribution, x_0, x_1, x_2, for diamond at 100 K, the average number of e-h pairs per drop, $\bar{n}$ and the relative mean square of the droplet distribution $\overline{(\Delta n)^2}$ under different excitation. We use Gaussian pulse excitation with $t_p = 0.1$ ps and $t_0 = 0.1$ ps: (a) $G_0 = 6 \times 10^{30}$ cm^{-3} s^{-1}; (b) $G_0 = 20 \times 10^{30}$ cm^{-3} s^{-1}.

density of all e-h pairs which are condensed into droplets, x_1, is much larger—around 10^{18} cm^{-3} which is at least four orders of magnitude larger.

The high excitation creates a large number of excitons, which then produce a large number of small droplets. However this process, together with the growth of the newly created small droplets, tend to reduce n_x. As n_x becomes smaller, the thermal potential in Eq. (A1) forms a higher barrier between excitons-multiexciton complexes and EHDs.[22,23] When the thermal potential grows high enough, it blocks the multiexciton complexes to grow into small droplets and the reverse process. Thus for a relatively long time, the droplet density x_0 becomes stable. It is noted that x_0 always becomes stable before other moments, x_1 and x_2, get stable as shown in Figs. 5(a) and 5(b).[12,21] Thus the formation process is separated into two stages: The first is the process of the growth of the number of droplets; and the second is the process of the growth of the size of the droplets. From Fig. 5(a) one can see that the first stage ends at about 8×10^3 ps, and the second one ends at 2×10^4 ps. The formation process after the first stage is a key one for the growth of the size of droplets. In Fig. 5(a) one can see that n_x stays nearly unchanged during this process, because the number of droplets is very small and the growth of these droplets requires very few excitons. In this case the thermal potential in Eq. (A1) remains nearly the same so that there is enough time for the e-h system to evolve slowly into its equilibrium, where the average drop size is very large, while in Fig. 5(b) one finds the process in 80–200 ps causes n_x to decrease by one order of magnitude. The depletion of excitons prevents droplets to grow larger, i.e., the shortage of excitons stops the growth of the size of droplets when the gain g_n and loss l_n rates are equal. Therefore the system can only reach a steady state which is in fact far away from equilibrium. It is noted from Eq. (7) that $n_c \propto (\ln n_x)^{-3}$, i.e., n_c decreases with the increase of excitation. This, together with the fact that the formation rates of multiexciton complexes are proportional to n_x, tend to increase the number of small droplets greatly with the increase of excitation density. In short, a large excitation tends to create too many small droplets which are unable to grow into large ones due to the limited number of excitons. And as a result, the density of exciton, n_x, is small while the density of all e-h pairs condensed in droplets, x_1, is large. These metastable features are similar to those in Ge at a high enough temperature.[21]

In summary we have studied the kinetics of EHD formation and decay at low (12 K) and high (100 K) temperatures under both low and high excitations by master equations. At low temperature our results are comparable with measurements reported by Nagai *et al.*[8] The time evolution of exciton and EHD basically represents the time-resolved photoluminescence measurement. The possible causes of the discrepancies between the calculation and the experiments are discussed in detail. The ANPC under both low and high excitation are too small to form macroscopic EHDs. The smallness of ANPC and the time during which the system is in equilibrium indicate that the phase transition is a second order process as in direct semiconductors. Despite much simplification in the model of the master equation theory, our results are in good qualitative agreement with experimental results. Our study of EHD at high temperature predicts that the average drop size is as large as 10^6. Moreover, under low excitation the average size of EHDs is very large but the EHD density is very low. Under high excitation the average size of EHDs is much smaller, but the EHD density is much larger. The physics behind these predictions is discussed in detail. These effects demonstrate the metastable feature of the kinetics at high temperature in diamond. Experiments are needed to verify these predictions.

This work was supported by the Natural Science Foundation of China under Grant No. 90303012, Anhui Provincial Natural Science Foundation and SRFDP. M.W.W. was also supported by the "100 Person Project" of Chinese Academy of Sciences and the Natural Science Foundation of China under Grant No. 10247002. M.K.G. acknowledges JSPS, KAKENHI (S) and SORST program from JST for financial support. The authors gratefully acknowledge the critical reading of this manuscript by Dr. Jean Benoit Heroux. J.H.J. would like to thank L. Jiang for valuable discussions.

APPENDIX: THE EXPRESSIONS OF J_{n_c} AND $f(n_c,t)$

The probability current from droplets J_{n_c} in Eq. (8) is given by Staehli:[21]

$$J_{n_c} \approx b n_x n_c^{2/3}\left[\frac{F_x(n_c)}{p} - \left(\frac{n_c}{\overline{n}}\right)^{3/2}\frac{C}{p}\exp\left(\frac{\Psi(\overline{n}) - \Psi(n_c)}{kT}\right)\right], \tag{A1}$$

with $F_x(n) = n_x n^{3/2}\exp[-\Psi(n)/kT]$ denoting the distribution function of excitons and multiexciton complexes. $p = \sqrt{2\pi kT/[\partial^2\Psi(n)/\partial n^2]_{n_c}}$ is the width of the potential barrier between excitons/multiexciton complexes and EHDs. $\overline{n} = x_1/x_0$ is the average drop size. $C = x_0/[2\int_{n_c}^{n}(n/\overline{n})^{3/2}\exp(\Psi(\overline{n}) - \Psi(n)/kT)dn]$ is a normalization factor of the distribution function of EHDs and the thermal potential $\Psi(n)$ is given by[23]

$$\Psi(n) = -kTn\ln\frac{n_x}{n_s} + 4\pi R_0^2\sigma n^{2/3} + kT\sum_{j=1}^{n}\ln\left(1 + \frac{j}{\alpha_j\tau_d}\right). \tag{A2}$$

As for $f(n_c,t)$, when $\partial n_c/\partial t > 0$ it takes the form of distribution function of excitons and multiexciton complexes:

$$f(n_c,t) \approx F_x(n_c)/2. \tag{A3}$$

Otherwise, it takes the form of distribution function of EHDs:

$$f(n_c,t) \approx C\left(\frac{n_c}{\overline{n}}\right)^{3/2}\exp\left(\frac{\Psi(\overline{n}) - \Psi(n_c)}{kT}\right). \tag{A4}$$

*Author to whom correspondence should be addressed. Electronic address: mwwu@ustc.edu.cn
†Mailing address.

[1] *Electron-Hole Droplets in Semiconductors*, edited by C. D. Jefferies and L. V. Keldysh (North-Holland, Amsterdam, 1983).
[2] R. M. Westervelt, *Electron-Hole Droplets in Semiconductors* (Ref. 1), Chap. 3.
[3] S. W. Koch and H. Haug, Phys. Lett. **74A**, 250 (1979).
[4] M. Combescot and R. Combescot, Phys. Lett. **56A**, 228 (1976).
[5] R. Shimano, M. Nagai, K. Horiuch, and M. Kuwata-Gonokami, Phys. Rev. Lett. **88**, 057404 (2002).
[6] K. Thonke, R. Schliesing, N. Teofilov, H. Zacharias, R. Sauer, A. M. Zaitsev, H. Kanda, and T. R. Anthony, Diamond Relat. Mater. **9**, 428 (2000).
[7] R. Sauer, N. Teofilov, and K. Thonke, Diamond Relat. Mater. **13**, 691 (2004).
[8] M. Nagai, R. Shimano, K. Horiuchi, and M. Kuwata-Gonokami, Phys. Rev. B **68**, 081202(R) (2003).
[9] M. Nagai, R. Shimano, K. Horiuch, and M. Kuwata-Gonokami, Phys. Status Solidi B **238**, 509 (2003).
[10] H. Haug and F. F. Abraham, Phys. Rev. B **23**, 2960 (1981).
[11] R. N. Silver, Phys. Rev. B **11**, 1569 (1975); **12**, 5689 (1975); **16**, 797 (1976).
[12] S. W. Koch and H. Haug, Phys. Status Solidi B **95**, 155 (1979).
[13] The boundary temperature T_b can also be evaluated by scaling: For Si, T_b is approximate 9 K and the work function $\phi = 95.1$ K. For diamond, $\phi = 580$ K and the recombination rate is 150 times as large as that of Si. Therefore from $T_b^2 \times \exp(-\phi/kT_b)|_{\text{diamond}} = 150 \times T_b^2\exp(-\phi/kT_b)|_{\text{Si}}$, we conclude $T_b|_{\text{diamond}} \approx 60$ K.
[14] We assume 100 ns for exciton lifetime in our calculation. Exciton lifetime depends on the temperature, excitation density, and sample quality—because lifetime is mainly determined by impurity-related nonradiative processes. However the simulation including these effects is too complicated. We use the approximation of 100 ns, which does not make essential difference in the time region of about 100 ns.
[15] This is the work function at 100 K. The work function at 12 K may be smaller as the experiment by Sauer *et al.* (Ref. 7) suggested. However, even if one takes the work function at 12 K as one-half of that at 100 K to evaluate evaporation rate at 12 K, the calculation shows that the evaporation rate at 12 K is so small that one can drop the evaporation term in the calculation.
[16] We get this value by fitting the time when density x_1 reaches maximum under the excitation intensity of 4 mJ/cm^2 at 100 K as approximately the same as that of 121 K under same excitation which is shown in Fig. 4(d) of R. Shimano, M. Nagai, K. Horiuch, and M. Kuwata-Gonokami, Phys. Rev. Lett. **88**, 057404 (2002).
[17] We assume that the excitation density depends linearly on exciting laser intensity with $G_0 = I_x \times 0.33 \times 10^{31}$ cm^{-3} s^{-1}, where I_x is excitation intensity in mJ/cm^2 (the coefficient 0.33×10^{31} cm^{-3} s^{-1} is obtained by fitting n_{Mott} to exciting laser intensity 6.9 mJ/cm^2 in Fig. 4. of Ref. 8).
[18] L. Jiang, M. W. Wu, M. Nagai, and M. Kuwata-Gonokami, Chin. Phys. Lett. **20**, 1833 (2003).
[19] M. Nagai and M. Kuwata-Gonokami, J. Phys. Soc. Jpn. **71**, 2276 (2002).
[20] R. B. Hammond and R. N. Silver, Phys. Rev. Lett. **42**, 523 (1979).
[21] J. L. Staehli, Phys. Status Solidi B **75**, 451 (1976).
[22] R. M. Westervelt, Phys. Status Solidi B **76**, 31 (1976).
[23] R. M. Westervelt, Phys. Status Solidi B **74**, 727 (1976).